Dynamics of Multisoliton Interactions in Parametrically Resonant Systems

Xinlong Wang and Rongjue Wei
Institute of Acoustics, Nanjing University, Nanjing 210093, People's Republic of China
(Received 9 July 1996)

Several important dynamical aspects of parametrically excited multisolitons are observed experimentally and further simulated with the parametrically driven, damped nonlinear Schrödinger equation. These aspects include the three basic modes of soliton-soliton interactions, the chaotic motions of the solitons, and transitions among different soliton states. [S0031-9007(97)02866-4]

PACS numbers: 43.25.+y, 47.20.Ky, 47.35.+i

A class of nonlinear resonant phenomena in various physical media are described by the *parametrically driven, damped nonlinear Schrödinger equation* (PDNLS) [1]

$$i(\phi_\tau + \alpha\phi) + \phi_{XX} + 2|\phi|^2\phi + \gamma e^{-2i\beta\tau}\phi^* = 0, \tag{1}$$

or by the autonomous one

$$i(\psi_\tau + \alpha\psi) + \psi_{XX} + (\beta + 2|\psi|^2)\psi + \gamma\psi^* = 0, \tag{2}$$

where $\psi(X,\tau) = e^{i\beta\tau}\phi(X,\tau)$. These phenomena include the Faraday resonance in fluid dynamics [2,3], localized structures in nonlinear lattices [4], self-localized structures in granular materials [5], parametric generation of spin waves in ferro- and antiferromagnets [6], instabilities in plasma [7], and amplitude modulation in Josephson junction [8]. In all these cases, a suitable parametric excitation of the system can generate and sustain a solitonic wave, known as the *parametrically excited* (PE) *soliton*, a type of which was realized in an oscillating water tank [9]. In the absence of a parametric drive, i.e., $\gamma\exp(-i\beta\tau)\phi^* = 0$, Eq. (1) is nothing but the nonlinear Schrödinger (NLS) equation with linear damping. The introduction of the drive not only balances the energy dissipation but also determines the distinct nature of the soliton. For example, a single soliton is never propagating [9], and it can exhibit various bifurcation and chaotic behaviors in some parameter regions [1].

More than one PE soliton has already been observed in an oscillating channel [9,10], each being identical but with different polarities. However, the dynamic problems about multisolitons, especially the soliton-soliton interactions, still remain unclear or unresolved so far. The objective here is to explore these problems. Referring to the polarities, we shall use symbols "↑" and "↓" to denote a positive and negative polarity, respectively. For example, $S(\uparrow\uparrow)$ stands for the double solitons of like polarity, and $S(\uparrow\downarrow)$ for the double solitons of opposite polarity, etc.

We carry out our experiments by using an oscillating water trough [9,10]. The trough is made of Plexiglas and contains pure water in the region: $0 < x < l$, $0 < y < b$, and $-h < z < 0$ ($l \gg b, h$). Under a vertical drive, it oscillates in the simple form $z_0 = a_d\cos(2\omega t)$, where a_d and $f_d = \omega/\pi$ are the driving amplitude and frequency, respectively. In order to make the soliton formations easier, we have minimized the water surface tension coefficient down to about 37.6 dyne/cm^2. In this implementation, PE solitons appear as some surface cross waves but modulated with solitary-wave envelopes in the x direction [9]. The governing equation for the envelopes, i.e., Eq. (2), has been derived by Miles [2]. Let $k = \pi/b$, $T = \tanh(kh)$, and $\kappa = 2k\sqrt{T/[T + kh(1 - T^2)]}$, and assume ϵ is a small parameter ($0 < \epsilon \ll 1$) that measures the strength of nonlinearity. Then, in Miles's theory, (x,t) is mapped to (X,τ) in Eq. (2) as $\tau = \epsilon^2\omega t$ and $X = \epsilon\kappa x$, and (f_d, a_d) is related to (β,γ) as

$$\beta = \frac{\omega^2 - \omega_{01}^2}{2\omega^2\epsilon^2}, \qquad \gamma = \frac{\omega^2 a_d}{g\epsilon^2}, \tag{3}$$

where g is the acceleration of gravity, and $\omega_{01} = \sqrt{gkT}$ the linear eigenfrequency of the transverse mode $(0,1)$. For the details as well as the incorporation of the water surface tension, readers are referred to Miles's work [2].

We first describe the experimental results for $S(\uparrow\uparrow)$. As already reported [9,10], the double solitons of like polarity will interact with each other in a repeated sequence of attractions, collisions, and repulsions. For example, Fig. 1 shows the interactions and motions at the parameters $l \times b \times h = 20 \times 2.5 \times 2$ cm^3, $a_d = 0.75$ mm, and $f_d = 10.06$ Hz. We shall refer to this interaction pattern as M-I. A few of the new facts are further observed in our recent inspection. When a_d is decreased to certain value, $S(\uparrow\uparrow)$ will degenerate into $S(\uparrow)$. On the other hand, as a_d increases, the oscillation diminishes and each soliton becomes standing. In a very long trough, e.g., $l \times b \times h = 40 \times 3 \times 2$ cm^3, the oscillating pair becomes unstable due to the excitations of other surface-wave modes, but the unwanted excitations may be greatly suppressed by adding some absorbent, such as cotton, on both end walls, which leads to the pair more stable. Obviously, the oscillation mode is internal to $S(\uparrow\uparrow)$. In a sense, $S(\uparrow\uparrow)$ is of a "*bound state*," or "*bound-pair*."

By contrast, the behaviors of $S(\uparrow\downarrow)$ are quite different. Two distinct dynamical modes are observed. One is found in a shorter trough, e.g., $l \times b \times h = 20 \times 3 \times 2$ cm^3. Figure 2(b) shows the interactions and oscillations (M-II) under a drive, say, $f_d = 9.7$ Hz and $a_d = 0.8842$ mm.

 0031-9007/97/78(14)/2744(4)$10.00

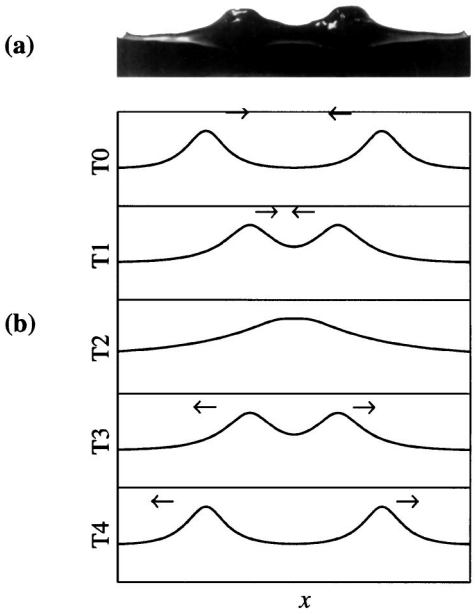

FIG. 1. Interactions and motions of the double solitons $S(\uparrow\uparrow)$. (a) Photo; (b) M-I in a period: $T0 \rightarrow T4$.

In this mode, both solitons oscillate *in phase* in the x direction, with a period about 10 s. Once a soliton collides on its nearby end wall, the other must be away from the other end wall, and they soon change their directions of motions. In this case, $l \sim 2\lambda$, where λ is the extension of a soliton ($\lambda \sim 7$ cm), and considerable parts of the solitary-wave envelopes overlap. Thus the behavior should result from the tight coupling between the solitons, as well as the strong boundary effect [10]. The other mode (M-III) is observed in a longer trough, say, $l \times b \times h = 40 \times 3 \times 2$ cm^3. A careful observation shows that there always exists a repulsion between the opposite polarity solitons; the closer they are, the stronger the repulsion is. Last, they are pushed close to the two end walls, respectively, and are eventually "captured" by the boundaries in a long term evolution, *typically several hours or even more than one day.* In the final steady state, they are separated by approximately 32 cm, so there is a little overlap in between. As expected, each soliton would behave as a boundary one, which has been reported earlier [10]. What surprises us here is the synchronous oscillations between the *weakly coupled* solitons, which, as opposed to M-II, are *exactly* 180° *out of phase.* Figure 2(c) shows the interaction and motion (M-III) when $a_d = 0.819$ mm and $f_d = 9.7$ Hz. The oscillation period varies slightly with (a_d, f_d), and is typically 20 s. Both M-II and III exist only in limited ranges of (a_d, f_d). When a_d is decreased to a certain value, one of them or both will be attached to the end walls, displaying halves of the envelopes; while, at a large a_d, the solitons become standing.

It is found that the three modes are basic to the system and exist in many other multisoliton states. For instance, the 4-soliton state $S(\uparrow\downarrow\downarrow\uparrow)$ realized in a trough of $l \times b \times h = 30 \times 2.5 \times 2$ cm^3 will oscillate in a pattern

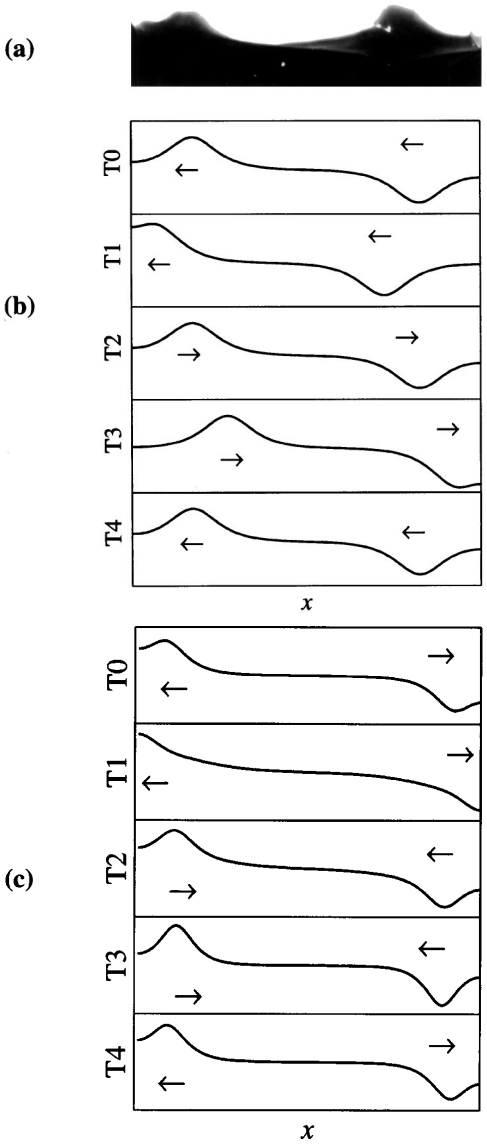

FIG. 2. Interactions and motions of the double solitons $S(\uparrow\downarrow)$. (a) Photo; (b) M-II in a period: $T0 \rightarrow T4$; (c) M-III in a period: $T0 \rightarrow T4$.

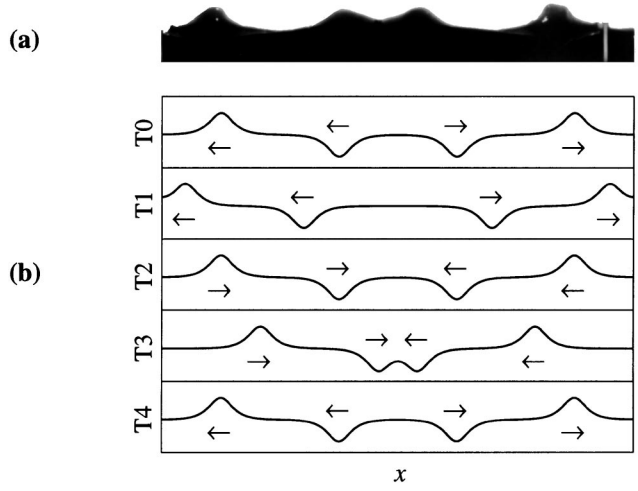

FIG. 3. Interactions and motions of the 4 solitons $S(\uparrow\downarrow\downarrow\uparrow)$. (a) Photo; (b) interactions in a period: $T0 \rightarrow T4$.

shown in Fig. 3 when $a_d = 1.25$ mm and $f_d = 11.0$ Hz. As we can see, this pattern is a simple combination of M-I and II. The similar situation also occurs in the states such as $S(\uparrow\uparrow\downarrow)$, $S(\uparrow\uparrow\downarrow\downarrow)$, and $S(\uparrow\uparrow\downarrow\downarrow\uparrow)$.

Could the PDNLS equation describe the observations above or even give us more information of the system in a more general sense? Owing to the nonintegrability, we attempt to answer the question here by invoking numerical solutions. We integrate Eq. (2) by using an implicit finite-difference algorithm with respect to X and the fourth order *Runge-Kutta-Fehlberg* algorithm with respect to τ. The boundary conditions $\psi_X|_{X=0,L} = 0$ are incorporated, where $L = \epsilon\kappa l$, and the computation error is controlled within 10^{-6}.

Our main results are summarized in Fig. 4. These are the stability diagrams in the (β, γ) plane for the three modes described above. For M-I, we present here the result for a relatively long trough ($L = 25.09$), in which the boundary effect is insignificant. On the diagrams, the point (1) corresponds to $l \times b \times h = 40 \times 3 \times 2$ cm^3, $a_d = 0.63$ mm, and $f_d = 9.7$ Hz when ϵ takes 0.3089, while (2) and (3) are the direct translations of the experimental parameters ($\epsilon = 0.3296$). Figure 5 shows the simulations at these points. Obviously, the computations reproduce the observations quite well.

In all these modes, if varying γ out of the stability regions, then the experimentally observed transitions and degenerations have been reproduced too, e.g., $S(\uparrow\uparrow) \rightarrow S(\uparrow)$ at the lower bound of region (M-I). For M-II and III, a careful investigation further reveals the existences of some finer and complex nonlinear structures in the vicinity of the lower boundaries of the regions. As γ is gradually decreased, $S(\uparrow\downarrow)$ manifests itself as periodic $\rightarrow$ quasiperiodic $\rightarrow$ chaotic oscillation, and then, transits to a "1.5" soliton state, one being attached to a boundary. Plotted in Fig. 6 is the phase portrait on the third stage of the scenario. It is identified as a strange attractor, signifying the onset of chaos.

For better understanding of the soliton dynamics, we have further inspected several dynamical quantities,

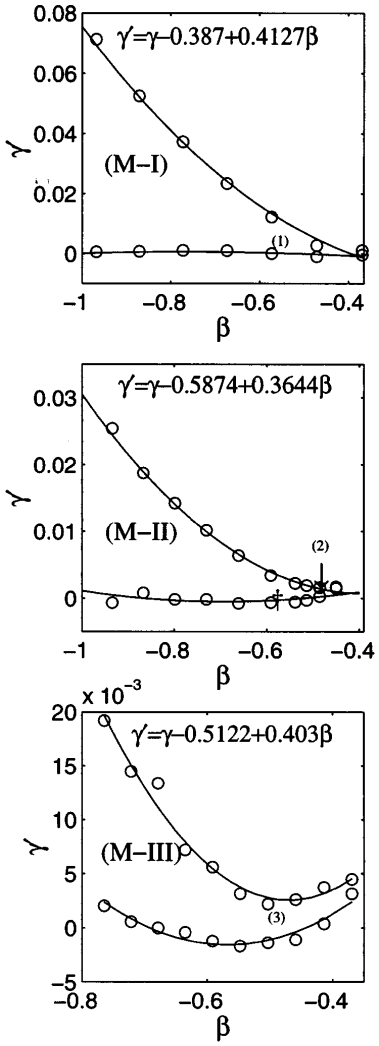

FIG. 4. The parameter regions for M-I, II, and III, respectively. (M-I) $L = 25.09$, $\alpha = 0.4519$; (M-II) $L = 12.55$, $\alpha = 0.5896$; (M-III) $L = 25.09$, $\alpha = 0.5896$.

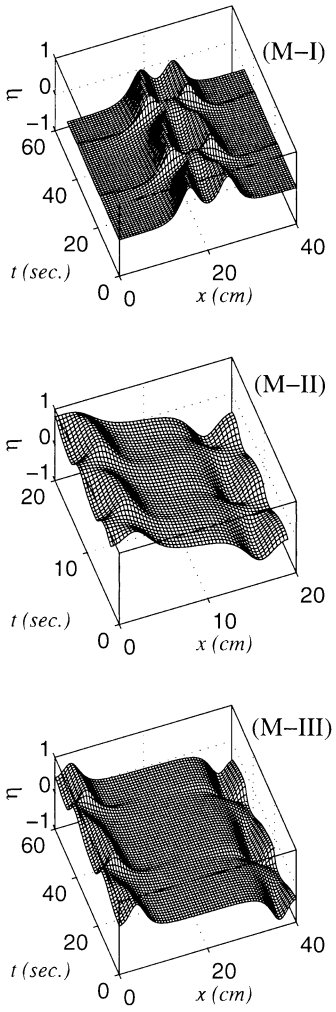

FIG. 5. Simulations of the three modes at the points denoted by (1), (2), and (3) in Fig. 4 [$\eta = \mathrm{Im}(\psi)$].

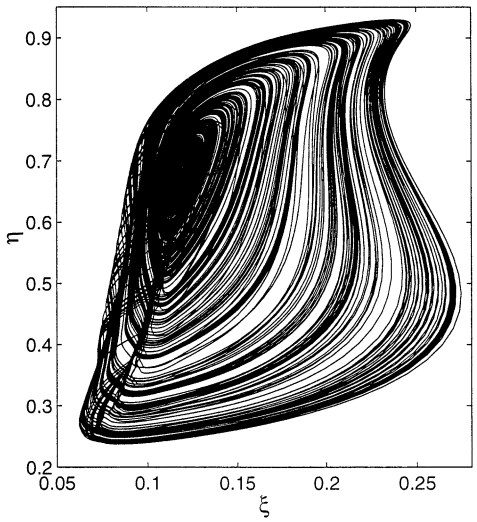

FIG. 6. Phase trajectory of $S(\uparrow\downarrow)$ at the point "†" in Fig. 4 (M-II), where $(\beta, \gamma) = (-0.5192, 0.8018)$ $[\xi = \mathrm{Re}(\psi), \eta = \mathrm{Im}(\psi)]$.

namely, the "particle" number N, momentum M, and energy E. They are formulated as

$$\begin{aligned} N(\tau) &= \int_0^L |\psi(X,\tau)|^2\, dX\,, \\ M(\tau) &= \int_0^L \mathrm{Im}(\psi^* \psi_X)\, dX\,, \\ E(\tau) &= \frac{1}{2}\int_0^L [\beta|\psi|^2 + \gamma \mathrm{Re}(\psi^2) \\ &\qquad + |\psi|^4 - |\psi_X|^2]\, dX\,. \end{aligned} \tag{4}$$

These quantities are conservative for the NLS solitons, but for the PDNLS equation (2), it follows from (4) that

$$\begin{aligned} \Delta_\tau N &= 2\gamma \int_0^L \mathrm{Im}(\psi^2)\, dX\,, \\ \Delta_\tau M &= [|\psi|^4 + \tfrac{1}{2}(|\psi|^2)_{XX}]_0^L, \\ \Delta_\tau E &= -\alpha \int_0^L |\psi|^4 dX\,. \end{aligned} \tag{5}$$

where $\Delta_\tau \equiv \left(\frac{d}{d\tau} + 2\alpha\right)$. As we can see, in general, N, M, and E vary with τ. For instance, as $\psi(\,,\tau)$ is periodic for the three modes, N and E are clearly periodic too as $\tau \to \infty$. For M-I and III, $M \to 0$ due to the symmetry of the motions, but for M-II, $M \neq 0$ as $\tau \to \infty$, and its direction changes alternately in the $\pm x$ direction. Figure 7 gives an example of the variations.

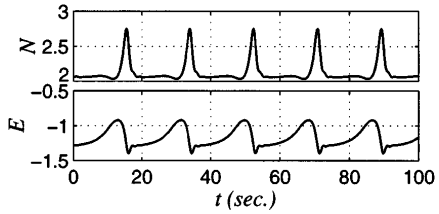

FIG. 7. Variations of N and E in the oscillating pair $S(\uparrow\uparrow)$ $(M = 0)$.

To summarize, many interesting behaviors of the PE solitons, in particular, the three basic dynamical modes, are revealed experimentally, and they are all confirmed by the simulations to Eq. (2). M-I is shown to be internal to $S(\uparrow\uparrow)$; while M-II and III in $S(\uparrow\downarrow)$ are the results of the dynamical balances between the repulsion of the solitons and the boundary influence. By applying the "mirror effect" [10], we see that $S(\uparrow\downarrow\downarrow\uparrow)$ is simply a periodic extension of $S(\uparrow\downarrow)$, and they are all equivalent to the periodic solitary-wave chain $S(\cdots\uparrow\downarrow\downarrow\uparrow\uparrow\downarrow\downarrow\uparrow\uparrow\downarrow\downarrow\uparrow\cdots)$ in an infinite waveguide. In the virtual state, every two neighboring solitons of like polarity would form a bound pair, acting as a classic "oscillator" (M-I). Depending on the strength of coupling, neighboring oscillators, with their polarities opposite to each other, would be locked either in phase (M-II) or 180° out of phase (M-III). Insufficient energy feed would have the oscillators out of steps, thus leading to chaos, and then, the collapse of one or more bound pairs.

The work is supported by the National Science Foundation of China (No. 19204008) and the State Key Lab. of Modern Acoustics of Nanjing University.

[1] Mariana Bondila, Igor V. Barashenkov, and Mikhail M. Bogdan, Physica (Amsterdam) **87D**, 314–320 (1995).
[2] J. W. Miles, J. Fluid Mech. **148**, 451 (1984).
[3] W. Z. Chen, R. J. Wei, and B. R. Wang, Phys. Lett. A **208**, 197–202 (1995).
[4] B. Denardo *et al.*, Phys. Rev. Lett. **68**, 1730–1733 (1992).
[5] W. Z. Chen, Phys. Lett. A **196**, 321–324 (1995).
[6] I. V. Barashenkov, M. M. Bogdan, and V. I. Korobov, Europhys. Lett. **15**, 113 (1991).
[7] N. Yajima and M. Tanaka, Prog. Theor. Phys. Suppl. **94**, 138 (1988).
[8] G. Cicogna and L. Fronzoni, Phys. Rev. A **42**, 1901 (1990).
[9] J. Wu, R. Keolian, and I. Rudnick, Phys. Rev. Lett. **52**, 1421–1424 (1984).
[10] X. L. Wang and R. J. Wei, Phys. Lett. A **192**, 1–4 (1994).